THE JOURNAL OF PHYSICAL CHEMISTRY B

Article

pubs.acs.org/JPCB

Role of Photoionization on the Dynamics and Mechanism of Photoinduced Electron Transfer Reaction of Coumarin 307 in Micelles

Namasivayam Dhenadhayalan and Chellappan Selvaraju*

National Centre for Ultrafast Processes, University of Madras, Chennai 600 113, India

Supporting Information

ABSTRACT: The dynamics and mechanism of the photoinduced electron transfer (PET) reaction between coumarin 307 (C307) and aromatic amines in micelles have been studied by using steady-state (S−S) and time-resolved (T-R) absorption and fluorescence spectroscopy. Based on the fluorescence quenching time scale, PET in micelles is grouped into two types: (i) ultrafast electron transfer (ET) due to the close contact of the donor and acceptor in micelles and (ii) diffusion averaged dynamic electron transfer (DADET) which is controlled by the diffusion of the reactants in micellar Stern layer and diffusion of the micelles. The DADET does not affect the photoionization and solvation processes whereas ultrafast ET competes with the photoionization and faster than the solvation process. Both ultrafast and DADET shows Marcus inversion in the ET rates at the similar exergonicity and indicates that the role of diffusion and solvent reorganization is negligible toward the activation barrier for the ET reaction in micelles. The activation barrier for the ET reactions in micelles is mainly due to intramolecular reorganization energy. The intramolecular reorganization energy must be higher in CTAB due to the photoionization and subsequent recombination and also involvement of triplet state in the PET. The ET reaction between coumarin radical cation and amine is reported for the first time in the C307-amine systems in micelles which are confirmed by the effect on amine concentration of the decay of coumarin radical cation and the dynamics of the ground-state recovery of C307. A mechanism for the PET reaction between C307−amine systems is proposed in micelles including photoionization, ultrafast and dynamic ET, and solvation dynamics.

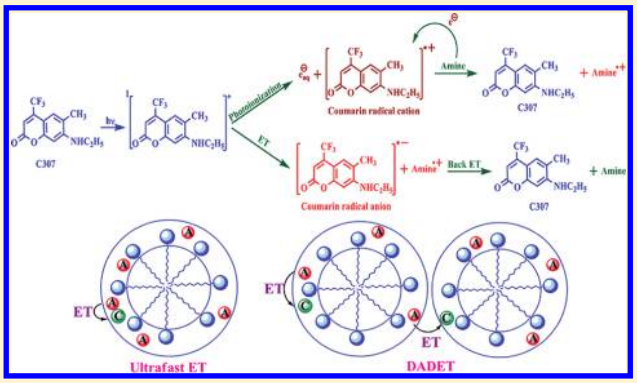

INTRODUCTION

Photoinduced electron transfer reactions in soft matters have attracted a lot of attention to investigate the effect of topology of the restricted geometry on the kinetics and mechanism of ET reactions. The soft matter systems are made up of molecular assemblies, which are self-organized; they have many different length scales from atomic (nanometers) to microscopic (millimeters) and their dynamics exhibit many different time scales from femtosecond to hours. The well-established soft matter systems include micelles, reverse micelles, vesicles, liquid crystals, cyclodextrins, polymers, and so on.[1,2] The PET reaction between donor and acceptor moieties plays a significant role in solar energy conversion and storage devices.[3−5] The separation distance between the ionic substrates must be larger to achieve the formation of long-lived ion pairs. Due to the multiphase character and constrained geometries, micelles and vesicles have been proved to be useful media in isolating the radical ions produced in ET reactions by slowing down the rate of geminate recombination and increasing the overall yield of the forward process. Moreover, the ET process in micellar systems can be considered as a model to gain insight into electron transport occurring in biological phenomena.

The dynamics of the PET reaction in micellar solutions depends on the micellar characteristics and attracts considerable interest for two reasons.[6−9] First, the close proximity of donor and acceptor molecules in micelle leads to very fast ET, and second, the ET occurs faster than the solvation process. Previously, it has been emphasized that the solvation dynamics and PET are competitive processes.[6−9] Yoshihara et al. first reported the ultrafast ET decay component, which is faster than the solvation time in neat donors (amines) as solvent.[10−13] Akesson et al.[14] have reported that the ultrafast PET in betaine dyes is completely decoupled from solvation. Bagchi et al. have reported interplay between ultrafast polar solvation and vibrational dynamics in ET reactions, the role of high-frequency vibrational modes, and also the effects of ultrafast solvation on the rate of adiabatic outer-sphere ET reactions.[15,16] Ghosh et al. reported the nondiffusive nature of the ET interactions by

Received: February 12, 2012
Revised: March 21, 2012
Published: April 9, 2012

dx.doi.org/10.1021/jp301412c | J. Phys. Chem. B 2012, 116, 4908−4920

ultrafast fluorescence quenching experiments in CTAB micelles.[17] Nevertheless, there are more aspects of the bimolecular ET reactions in soft matters that remain unexplored at pico- and femtosecond time scales. Therefore it is important to understand the relationship between the observed ET rate constants at different time scales and the nature of the micellar microenvironments on different ET components.

The significant aspects of ET studies are the understanding of the inversion in the ET rates at higher exergonicity, which are universally known as the Marcus inversion.[18−23] Several reports in the literature have been aimed at understanding the various aspects of ET dynamics in micellar media, especially the inversion behavior in the high exergonicity region.[23−26] So far, several authors have reported that solvent reorganization plays a significant role in the observed higher exergonicity in the Marcus inversion.[24−26] Chakraborty et al. have suggested that inversion for bimolecular ET rates in a micellar media at higher exergonicity is a result of slower diffusion of the probes in the micellar phase.[27] Yoshihara et al. observed a Marcus inverted bell shaped dependence of the rate of ET on free energy change even when ET is faster than solvation.[11−13]

Recently, many research groups have investigated the PET reaction of coumarin dyes with amines in soft matters such as micelles and ionic liquids using S-S and T-R fluorescence techniques.[28−31] The detailed understanding of the various aspects of ET dynamics in micellar media especially the ultrafast ET components and influence of solvation on ET reaction was discussed and reported recently.[8,9,28−31] The numerous important facets of the reaction mechanism of ET in organized media remain unveiled. To the best of our knowledge, there is no report to provide evidence for ET reaction between coumarin and amines in micellar medium by characterizing the transient species produced by ET such as amine radical cation, coumarin radical anion, and the transient species produced by the excited-state photochemical reaction of coumarin. In the present investigation, the nanosecond transient absorption measurements have been carried out to establish the mechanism and dynamics of the ET reaction along with T-R fluorescence studies. On excitation, C307 undergoes photoionization which results in the formation of hydrated electron and coumarin radical cation in all micelles. The effect of photoionization and ion-pair recombination on solvation dynamics was reported by our group.[32] In the present report, the effect of photoionization of C307 on the PET in micelles is explored. The PET in micelles are grouped into two classes: (i) ultrafast ET due to the close contact of the donor and acceptor in micelles and (ii) diffusion averaged dynamic ET which is controlled by the diffusion of reactant in micelles and diffusion of the micelles. Ultrafast ET competes with the photoionization and solvation dynamics whereas the slow dynamic ET does not affect the photoionization and solvation dynamics. In the present study, the C307 dye used as electron acceptor and aromatic amines such as aniline (AN), *N*-methylaniline (MAN), *N*-ethylaniline (EAN), *N*,*N*-dimethylaniline (DMAN), and *N*,*N*-diethylaniline (DEAN) are used as electron donors. Chemical structures of C307 and aromatic amines used in this study are shown in Scheme 1.

Scheme 1. Structure of the C307 and Amines Used in the Present Study

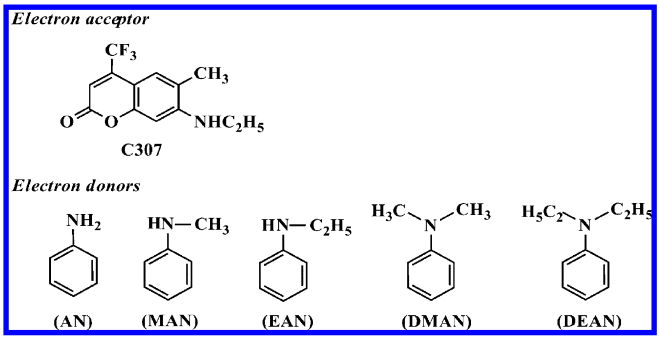

EXPERIMENTAL SECTION

Laser grade C307 was purchased from Exciton and used as received. Surfactants SDS and CTAB were of molecular biology grade purchased from SRL and Lancaster chemicals, respectively. TX-100 was purchased from Aldrich and all surfactants were used without any purification. Triply distilled water was used to prepare micellar solutions. Amines were purchased from SRL and Aldrich chemicals and were purified by vacuum distillation just before use.

The absorption spectra of the samples were recorded using an Agilent 8453 UV−visible diode array spectrophotometer. The fluorescence spectral measurements were carried out using a Fluoromax-4 spectrophotometer (Horiba Jobin Yvon). Time-resolved picosecond fluorescence decays were obtained by the time-correlated single-photon counting (TCSPC) technique with microchannel plate photomultiplier tube (Hamamatsu, R3809U) as detector and femtosecond laser as an excitation source. The second harmonics (400 nm) output from the mode-locked femtosecond laser (Tsunami, Spectra physics) was used as the excitation source. The instrument response function for TCSPC system is ∼50 ps. The data analysis was carried out by the software provided by IBH (DAS-6), which is based on reconvolution technique using nonlinear least-squares methods.

Femtosecond fluorescence transients have been collected using fluorescence up-conversion technique. In our femtosecond up-conversion setup (FOG 100, CDP, Russia) the sample was excited using the second harmonic (400 nm) of a mode-locked Ti-sapphire laser (Tsunami, Spectra physics). The fundamental beam (800 nm) was frequency doubled in nonlinear crystal (1 mm BBO, θ = 25°, ϕ = 90°) and used for the excitation. The sample was placed inside a 1 mm-thick rotating quartz cell. The fluorescence emitted from the sample was up-converted in a nonlinear crystal (0.5 mm BBO, θ = 38°, ϕ = 90°) using the fundamental beam as a gate pulse. The up-converted light is dispersed in a monochromator and detected using photon counting electronics. The instrument response function of the apparatus is 300 fs. The femtosecond fluorescence decays were fitted using a Gaussian shape for the excitation pulse. The femtosecond fluorescent decay was analyzed by fixing the longer lifetime component obtained from TCSPC.

Transient absorption experiments were carried out using nanosecond laser flash photolysis (Applied Photophysics, U.K.). The third harmonic (355 nm) of a Q-switched Nd:YAG laser (Quanta-Ray, LAB 150, Spectra physics, U.S.A.) with 8 ns pulse width and 150 mJ pulse energy was used to excite the sample. The transients were probed using a 150 W pulsed Xenon lamp, a Czerny-Turner monochromator, and Hamamatsu R-928 photomultiplier tube as detector. The transient signals were captured with an Agilent infiniium digital storage oscilloscope and the data were transferred to the computer for further analysis. For laser flash photolysis studies,

dx.doi.org/10.1021/jp301412c | J. Phys. Chem. B 2012, 116, 4908−4920

samples were purged with argon gas for 45 min prior to the laser irradiation.

The oxidation and reduction potentials in the micellar media exhibit a general shift from those in acetonitrile.[9,17] The oxidation potentials of the amines [E(D/D$^+$)] in micellar solutions versus SCE were estimated from the reported values in acetonitrile solution after applying a suitable correction for the micellar media.[9,13,17] The reduction potential of the coumarin dyes [E(A/A$^-$)] in acetonitrile solution was measured by the cyclic voltammetric (CV) method using a CH-620B instrument. Solution of C307 in acetonitrile containing 0.1 M TBAP as the supporting electrolyte was deaerated by high purity N_2 gas for about 15 min. CV measurements were then carried out using glassy carbon as the working electrode, Pt wire as the counter electrode, and silver−silver chloride [Ag/AgCl/Cl$^-$ (saturated)] as the reference electrode. We used a shift factor of 0.16, 0.44, and 0.13 V from the potentials in acetonitrile respectively for SDS, CTAB, and TX-100 micelles.[9,17]

In the present study, the concentrations of SDS, CTAB, and TX-100 were kept at 60 mM which is well above the critical micellar concentration (CMC). The micellar concentration was estimated from the surfactant concentration used, and the values of their CMC and aggregation numbers. The CMC of the surfactants SDS, CTAB, and TX-100 are 8.30, 0.80, and 0.24 mM, respectively.[33−35] The average aggregation number of SDS, CTAB, and TX-100 micelles is 62, 92, and 100, respectively.[33−35] Coumarin dyes are reasonably soluble in the micellar solution. The coumarin concentration was always kept about ∼10 μM, such that not more than one C307 molecule can occupy in single micelle. Amine concentrations were used always higher than the micelle concentrations, and varied over a wide range. As the volume of each micelle is restricted by the micellar boundary, the effective concentration of amines in the micellar Stern/palisade layer is much higher than the total amine concentration used in the solution. Hence the effective concentration of amine was used for quenching analysis instead of total amine concentration. The effective quencher concentration in the micellar Stern/palisade layer was calculated using the following equation:[35−37]

$$[Q]_{eff} = \frac{N_{agg}[Q]_t}{V_{SL}\{[surf]_t - CMC\}} \quad (1)$$

where V_{SL} is the volume of micellar Stern/palisade layer and $[Q]_t$ is the total quencher concentration used in the solution. SDS, CTAB, and TX-100 surfactants form spherical micelles, with the micellar radii of 30, 21.7, and 50 Å and nonpolar core radii of 21, 14.7, and 25 Å, respectively.[35−37] Thus, the thickness of the Stern/palisade layer for the three micelles appear to be 9, 7, and 25 Å, respectively.[35−37] On the basis of the above micellar parameters, the volume of the Stern/palisade layer is estimated to be 44.75, 17.76, and 275.94 dm^3 mol^{-1} for SDS, CTAB, and TX-100 micelles, respectively.

RESULTS

Steady-State Fluorescence Quenching Studies. Steady-state absorption and fluorescence spectra of C307 were recorded in micelles and data are compiled in Table 1. The fluorescence maximum of C307 in all the micelles is blue-shifted as compared with that of water (λ_{emi} = 506 nm) which indicated that C307 is located in the less polar environment in micelles compared with bulk water. The observed fluorescence maximum of C307 in all micelles is close to the fluorescence maximum value reported in methanol (λ_{emi} = 493 nm), which indicates that the polarity of the microenvironment of C307 in all micelles resembles methanol. These results confirm that the C307 is located in Stern/palisade layer of the micelles.[32] In all micellar systems, the longer wavelength absorption band of C307 remains unaffected on the addition of amines. This indicates that there is no ground-state interaction between the C307 and amines used in the present investigation. On the addition of amines, the fluorescence intensity of C307 was quenched without change in the shape of the fluorescence spectra even in the presence of high concentration of amines in all micellar solutions. This indicates a strong interaction between the C307 and amines in the excited-state but excludes the exciplex formation as the intermediates. Figure 1 shows the fluorescence spectra of C307 in SDS micellar solution in the absence and presence of different concentrations of DEAN. The absorption spectra for this system are also given in the inset of Figure 1. The quencher aromatic amines are also resides in the Stern/palisade layer of the micelles.[35−37]

Table 1. Various Parameter Values of C307 in Micelles

parameters	SDS	CTAB	TX-100
λ_{abs} (nm)	401	405	398
λ_{emi} (nm)	498	498	494
E_{00} (eV)	2.72	2.71	2.79
E(A/A$^-$) (V)	−1.50	−1.22	−1.53
τ_0 (ns)	5.83	5.20	5.90

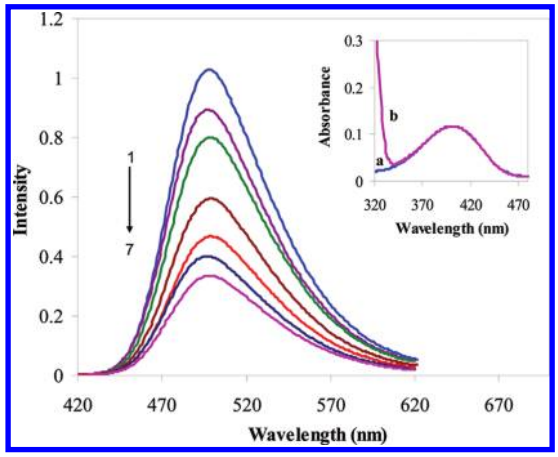

Figure 1. Fluorescence spectra of C307 in SDS micelle in the absence and presence of different concentrations of DEAN: (1) 0, (2) 4 × 10^{-4}, (3) 8 × 10^{-4}, (4) 16 × 10^{-3}, (5) 24 × 10^{-3}, (6) 32 × 10^{-3}, and (7) 40 × 10^{-3} M. The inset shows absorption spectra of C307 in SDS micelle in the absence (a) and presence (b) of DEAN.

Amines are very good electron donors, and coumarins are reported as electron acceptor in the excited-state.[11,12,35−37] The fluorescence intensity quenching of the C307 by the amines is attributed to the PET from amines to the excited C307. Bimolecular quenching rate constants for the ET process in micelles were determined by using the Stern−Volmer (S−V) relation

$$\frac{I_0}{I} = 1 + K_{s-v}[Q]_{eff} = 1 + k_q\tau_0[Q]_{eff} \quad (2)$$

where I_0 and I are the fluorescence intensity of C307 in the absence and presence of quencher, respectively. K_{s-v} is the

dx.doi.org/10.1021/jp301412c | J. Phys. Chem. B 2012, 116, 4908−4920

Stern–Volmer constant, k_q is the bimolecular quenching rate constant, τ_0 is the fluorescence lifetime of C307 in the absence of quencher, and $[Q]_{eff}$ is the effective concentration of quencher in the micellar phase. The S–V plot exhibits positive deviations from the linearity at higher amine concentration in all micelles. The representative S–V plot for the C307-amine systems in SDS micellar solution is shown in Figure 2. The

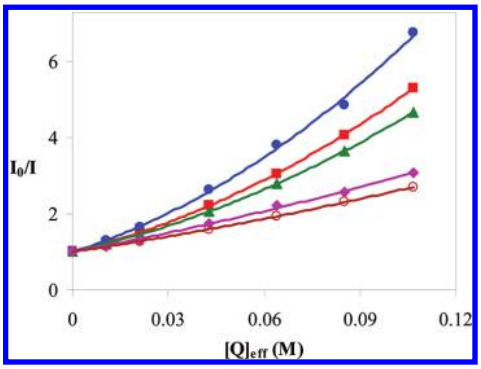

Figure 2. S–V plot for S–S fluorescence quenching of C307–amine systems in SDS micelles: AN (○), MAN (■), EAN (▲), DMAN (●), and DEAN (♦).

positive deviation from the linearity is due to the close proximity of some C307-amine pairs that leads to instantaneous quenching (static and transient quenching).[35,38,39] The steady-state quenching rate constants obtained using eq 2 at low effective quencher concentrations are compiled in Table 2. At low effective quencher concentration (0–0.04 M), the contribution of static and transient quenching is negligible and dependence of I_0/I is linear with quencher concentration.

Time-Resolved Picosecond Fluorescence Quenching Studies. The time-resolved fluorescence quenching studies were carried out by measuring the fluorescence decays of C307 at their emission maximum in the presence of amines to have a better understanding for ET in these systems. It is found that the fluorescence decays gradually become faster with increasing concentration of the amines. The fluorescence decays of C307 were fitted with single-exponential function in the absence of amine, whereas the decays were fitted by biexponential function in the presence of amines. Kumbhakar et al. reported that the quenching process in micellar media effectively occur under nondiffusive condition, and thus the ET kinetics in these systems is mainly determined by the distant-dependent distribution of the quenchers around fluorophores.[35–37] Since, the ET rate is distance-dependent, it introduces an inherent nonsingle exponential nature of the fluorescence decay in the presence of amines. In addition to this, contribution of diffusion of the reactants inside the micelles and micellar diffusion toward the quenching dynamics may result in the biexponential nature of the C307 fluorescence decay in the presence of amine. The micellar quenching model proposed by Infelta et al.[40] and Tachiya[41] is not followed in the present analysis due to the following reasons: (i) poor fit at higher concentration of the amines, (ii) slow diffusion of the reactants in the micellar Stern layer, (iii) micellar diffusion, and (iv) distance-dependent ET which affects the quenching constant per quencher occupancy. In the present work, we have adopted a similar approach used by Pal et al.[35–37,42] and Sarkar et al.[30] for analyzing the fluorescence decays, and the average fluorescence lifetime of the C307 in the presence of amines was used to obtain the quenching kinetics. The average lifetime of the C307 (τ_{av}) in the presence of different amine concentration was calculated using the following relation:[30,35–37,42]

$$\tau_{av} = A_1\tau_1 + A_2\tau_2 \quad (3)$$

where τ_1 and τ_2 are the fluorescence lifetimes of C307 and A_1 and A_2 are their relative amplitudes. For all C307–amine systems, it is seen that τ_{av} value gradually decreases with an increase in the amine concentrations. To estimate the rate constant for ET from time-resolved measurements using the S–V relation as[35–37]

$$\frac{\tau_0}{\tau_{av}} = 1 + k_q\tau_0[Q]_{eff} \quad (4)$$

where τ_0 is the fluorescence lifetime of the C307 in the absence of quenchers. The S–V plot shows linearity for all coumarin-amine systems in all micelles. The representative S–V plot for the C307–amine systems in SDS micelles is shown in Figure 3. The k_q values obtained from the T-R measurements in all micelles are also compiled in Table 2. It is seen that the k_q values obtained from the S–S fluorescence quenching measurements are higher than those obtained from the T-R quenching measurements. The close contact coumarin-amine pairs undergo static and transient quenching, which could not be detected with the present time resolution (~50 ps) of the TCSPC setup. In the T-R measurements using picoseconds TCSPC setup, the observed fluorescence decay is given the C307-amine pairs that are reasonably apart from each other as compared with the close proximity of C307-amine pairs, and thus shows the dynamic part of the quenching only. The higher k_q values obtained in the S–S measurements is due to static, transient and dynamic quenching processes, whereas k_q values obtained from the T-R measurements is due to the dynamic quenching alone. The static and transient quenching takes place

Table 2. Bimolecular Fluorescence Quenching Rate Constant (k_q) for the C307–Amine Systems in Micelles Obtained from S–S and T-R Fluorescence (TCSPC) Measurements

	k_q (10^9 M^{-1} s^{-1})[a]					
	SDS		CTAB		TX-100	
amines	k_q (S–S)	k_q (T-R)	k_q (S–S)	k_q (T-R)	k_q (S–S)	k_q (T-R)
AN	2.56	1.47	1.06	0.58	3.59	1.81
MAN	5.69	2.52	1.89	1.11	6.62	2.67
EAN	5.02	2.75	1.72	0.85	6.48	2.83
DMAN	5.79	2.58	1.20	0.82	7.32	2.69
DEAN	3.19	1.09	0.70	0.38	6.03	1.88

[a]Error: ±1%.

dx.doi.org/10.1021/jp301412c | J. Phys. Chem. B 2012, 116, 4908–4920

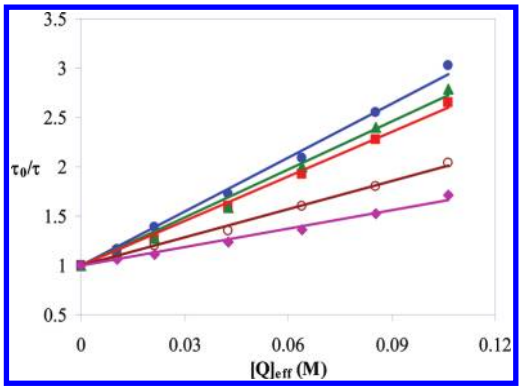

Figure 3. S−V plot for T-R fluorescence quenching of C307-amine systems in SDS micelles: AN (○), MAN (■), EAN (▲), DMAN (●), and DEAN (♦).

at a very fast time scale, i.e., in the subpicoseconds time scale, which is studied in the following section.

Ultrafast Fluorescence Quenching Studies. Femtosecond fluorescence decays of C307 in all micellar solutions were recorded at the blue end of the emission spectrum (460 nm) using femtosecond fluorescence up-conversion technique. On photoexcitation, the C307 molecule excited to the Franck−Condon state which is corresponding to the blue edge of the emission spectrum. The ultrafast ET competes with solvation dynamics, so that it can be studied only from the decay of the initially populated state rather than the relaxed state. The fluorescence decay of the relaxed state (monitored at red edge of the emission spectrum) shows rise component and the presence of rise component makes it very difficult to follow the ultrafast electron transfer from the relaxed state. Hence we have studied the ultrafast electron transfer by monitoring the fluorescence decay at the blue edge of the emission spectrum in all micelles. A typical ultrafast fluorescence decay of C307 in micelles in the absence and presence of different concentrations of DMAN is shown in Figure 4, and decay parameters are listed in Tables 3−5. The observed fluorescence decays are seen to be nonexponential in all micellar systems and are fitted satisfactorily by using a triexponential function. The ultrafast fluorescence decay of C307 was quenched with increasing concentration of amines. The fluorescence decay of C307 in all micelles have consist an ultrafast decay component (τ_1) of ~3 ps and the fast decay component (τ_2) of 50−70 ps along with a longer nanosecond decay component, detected in TCSPC measurements. In our previous work, we have reported the photoionization and solvation relaxation of C307 in micellar systems and photoionization of C307 occurs in the picosecond time scale (<30 ps) in all micelles.[32] Ghosh et al. have studied the ultrafast solvation dynamics in micelles using C480 probe and they reported the ultrafast solvation times of >3 ps in micelles.[9] Based on above results, the observed ultrafast decay component (τ_1) may be due to both photoionization and ultrafast solvation of C307 in the Franck−Condon state. The

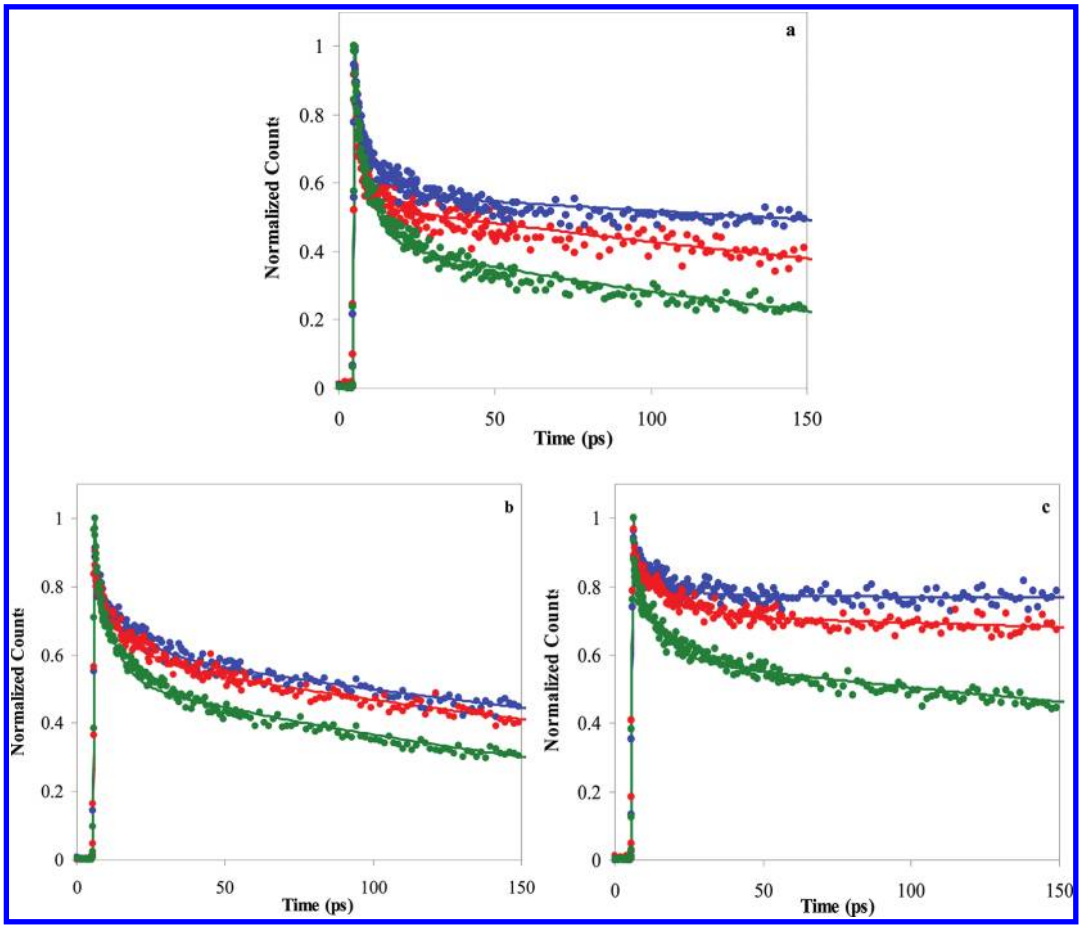

Figure 4. Femtosecond fluorescence decay of C307 in (a) SDS, (b) CTAB, and (c) TX-100 micelles monitored at blue edge with DMAN concentration of (●, blue) 0, (●, red) 3×10^{-3}, and (●, green) 15×10^{-3} M.

dx.doi.org/10.1021/jp301412c | J. Phys. Chem. B 2012, 116, 4908−4920

Table 3. Femtosecond Fluorescence Decay Parameters of C307 in SDS Micelles Monitored at 460 nm

amine	[amine] (mM)	$[amine]_{eff}$ (M)	τ_1/ps, $(a_1)^{a,c}$	τ_2/ps, $(a_2)^{a,c}$	τ_3/ns^b
AN	0	0	1.71 (0.33)	58.24 (0.67)	5.89
	3.25	0.0865	1.70 (0.58)	55.19 (0.42)	4.49
	15.02	0.4003	2.85 (0.49)	49.12 (0.51)	2.03
MAN	3.25	0.0865	4.22 (0.53)	51.94 (0.47)	3.99
	15.02	0.4003	1.63 (0.57)	38.38 (0.43)	1.25
EAN	3.25	0.0865	4.04 (0.53)	50.15 (0.47)	3.59
	15.02	0.4003	1.94 (0.56)	39.69 (0.44)	1.11
DMAN	3.25	0.0865	2.97 (0.56)	50.29 (0.44)	3.55
	15.02	0.4003	2.43 (0.60)	36.03 (0.40)	1.05
DEAN	3.25	0.0865	3.08 (0.57)	50.53 (0.43)	3.84
	15.02	0.4003	2.96 (0.50)	38.85 (0.50)	1.15

[a]Amplitudes are listed within parentheses; amplitude contribution was calculated from the initial decay components (τ_1 and τ_2) only, neglecting the contribution of long ns component. [b]From TCSPC setup. [c]Error ±10%.

Table 4. Femtosecond Fluorescence Decay Parameters of C307 in CTAB Micelles Monitored at 460 nm

amine	[amine] (mM)	$[amine]_{eff}$ (M)	τ_1/ps, $(a_1)^{a,c}$	τ_2/ps, $(a_2)^{a,c}$	τ_3/ns^b
AN	0	0	2.99 (0.37)	70.26 (0.63)	5.22
	3.25	0.2826	2.56 (0.52)	65.31 (0.48)	3.78
	15.02	1.3072	2.95 (0.49)	50.59 (0.51)	1.48
MAN	3.25	0.2826	4.12 (0.37)	62.02 (0.63)	3.43
	15.02	1.3072	2.08 (0.52)	44.38 (0.48)	1.13
EAN	3.25	0.2826	2.67 (0.50)	58.13 (0.50)	3.13
	15.02	1.3072	2.85 (0.48)	43.63 (0.52)	1.00
DMAN	3.25	0.2826	3.14 (0.40)	64.86 (0.60)	3.29
	15.02	1.3072	2.19 (0.52)	41.47 (0.48)	1.04
DEAN	3.25	0.2826	3.63 (0.47)	60.21 (0.53)	3.53
	15.02	1.3072	2.59 (0.49)	46.66 (0.51)	1.37

[a]Amplitudes are listed within parentheses; amplitude contribution was calculated from the initial decay components (τ_1 and τ_2) only, neglecting the contribution of long ns component. [b]From TCSPC setup. [c]Error ±10%.

Table 5. Femtosecond Fluorescence Decay Parameters of C307 in TX-100 Micelles Monitored at 460 nm

amine	[amine] (mM)	$[amine]_{eff}$ (M)	τ_1/ps, $(a_1)^{a,c}$	τ_2/ps, $(a_2)^{a,c}$	τ_3/ns^b
AN	0	0	5.05 (0.20)	63.41 (0.80)	5.23
	3.25	0.0195	1.74 (0.58)	57.71 (0.42)	4.67
	15.02	0.0906	3.12 (0.50)	52.31 (0.50)	3.39
MAN	3.25	0.0195	3.06 (0.49)	52.40 (0.51)	4.36
	15.02	0.0906	2.10 (0.51)	39.76 (0.49)	2.41
EAN	3.25	0.0195	2.22 (0.52)	52.06 (0.48)	4.23
	15.02	0.0906	1.87 (0.54)	39.60 (0.46)	2.31
DMAN	3.25	0.0195	1.26 (0.57)	53.54 (0.43)	4.11
	15.02	0.0906	2.28 (0.50)	37.27 (0.50)	2.40
DEAN	3.25	0.0195	4.19 (0.45)	56.91 (0.55)	4.05
	15.02	0.0906	3.66 (0.44)	48.87 (0.56)	2.65

[a]Amplitudes are listed within parentheses; amplitude contribution was calculated from the initial decay components (τ_1 and τ_2) only, neglecting the contribution of long ns component. [b]From TCSPC setup. [c]Error ±10%.

fast decay component (τ_2) is similar to the fast solvation component reported in the micelles,[32] and assigned to the solvation. In the presence of amine, there is not much change in the ultrafast decay component (τ_1) whereas the fast decay component (τ_2) gradually decreases with increasing concentration of amines. The decreasing fast decay constant clearly reveals that the ultrafast ET process competes with the solvation of the dye.

To confirm the existence of competition between the ultrafast ET and solvation, fluorescence decays were recorded at their red end of the emission spectrum (550 nm). In the absence of amine, the fluorescence decay at red end displays a rise component in all micelles which is due to solvent relaxation in the excited-state. The rise time observed at the decay monitored at 550 nm in all micelles was decreases on increasing amine concentration (Supporting Information, Figure S1). On increasing amine concentration, ET rate increases and competes with solvent relaxation processes. Using S−V analysis, the ultrafast ET rate constant (k_{et}) was calculated from the fast decay component (τ_2) monitored at 460 nm using the following equation:[39,43]

$$k_{et} = \frac{1}{\tau_2} - \frac{1}{\tau_0} \quad (5)$$

where τ_2 is the fast decay time constant of C307 in the presence of amine ([amine] = 15 mM) and τ_0 is the fluorescence lifetime of C307 in the absence of amine (which is taken from TCSPC). The ultrafast quenching rate constants in all micelles are found to be in the order of 2×10^{10} s^{-1} (Table 6). The determined ultrafast ET rate constants using a femtosecond setup are much higher than those observed in picosecond setup (TCSPC).

Table 6. Ultrafast Fluorescence Quenching Rate Constant (k_q) for the C307−Amine Systems in Micelles Obtained from Femto Up-Conversion Measurements

	k_q (10^{10} s^{-1})[a]		
amines	SDS	CTAB	TX-100
AN	2.02	1.96	1.99
MAN	2.59	2.23	2.50
EAN	2.61	2.27	2.51
DMAN	2.76	2.39	2.67
DEAN	2.56	2.12	2.13

[a]Error ±5%.

Time-Resolved Transient Absorption Studies. Evidence for the ET mechanism was obtained from the T-R transient absorption spectra of C307 in the presence of amines in all micellar systems. Transient absorption spectra of C307 in the presence of amines have been recorded in all micellar solutions on excitation at 355 nm under argon saturated conditions. In our previous work,[32] we have reported the transient absorption studies of C307 in micelles. The excited C307 undergoes photoionization resulting in the formation of the coumarin radical cation (λ_{max} at 610 nm) and hydrated electron (λ_{max} at 710 nm) in all micellar systems. In CTAB micelles, triplet−triplet absorption of C307 (λ_{max} at 590 and 710 nm) was observed, which is due to both the recombination of radical-ion pair and triplet induction by bromide counterions. On the contrary in TX-100 micelles, the recombination of the coumarin radical cation and hydrated electron results in the formation of the TICT state.[32]

dx.doi.org/10.1021/jp301412c | J. Phys. Chem. B 2012, 116, 4908−4920

In the presence of amines, the transient absorption spectrum shows a new transient absorption peak at 450−470 nm along with the board absorption in the wavelength range of 550−750 nm in SDS and TX-100 micellar systems. The representative transient absorption spectrum of C307 in the presence of DMAN in SDS micelles is shown in Figure 5. The observed

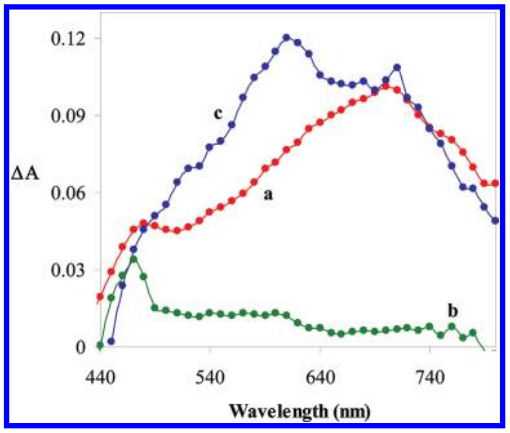

Figure 5. Transient absorption spectra of C307 in the presence of DMAN in SDS micelle under (a) argon and (b) N_2O saturated condition recorded at 1 μs after the laser pulse. Concentration of DMAN = 1.2×10^{-4} M. (c) Transient absorption spectrum of C307 in the absence of amine under argon saturated condition.

new transient peak (450−470 nm) is assigned as the absorption of the amine radical cation. The absorption of $MAN^{+\bullet}$ and $EAN^{+\bullet}$ is found to be in the region of 450 nm whereas the absorption of $DMAN^{+\bullet}$ and $DEAN^{+\bullet}$ is found to be in the region of 470 nm. The amine radical cation absorption reported in this work is found to be in good agreement with those reported in literature.[44,45] The absorption of amine radical cation confirms that the fluorescence quenching of C307 by amines is attributed to the ET from amine to C307. In the present studies, the observed transient absorption at 710 nm may be due to either the hydrated electron or coumarin radical anion. To confirm the transient responsible for the absorption in the range of 600−800 nm, the transient absorption spectrum of C307 with DMAN in the presence of electron scavenger (N_2O) was carried out. The transient absorption at 710 nm was found to disappear under N_2O saturated condition (Figure 5). This result reveals that the transient peak at 710 nm is due to the absorption of hydrated electron, and which is not due to the absorption of coumarin radical anion. The absorption due to neither coumarin radical cation nor coumarin radical anion was observed in the presence of amines. Now the question in front of us is, what happened to the (i) coumarin radical cation formed by the photoionization and (ii) coumarin radical anion formed by PET process. This suggests that after photoionization the coumarin radical cation and amine may be reacts to form the ground-state C307 molecule.

The decay kinetics for coumarin radical cation and hydrated electron were measured in SDS and TX-100 micelles as a function of amine concentrations. The representative transient decay of coumarin radical cation in TX-100 with different concentrations of EAN is shown in Figure 6. To the best of our knowledge, this is the first report on the study of interaction between coumarin radical cation and amines in micellar medium. It has been found that then lifetime and absorbance of coumarin radical cation decreases with increasing concen-

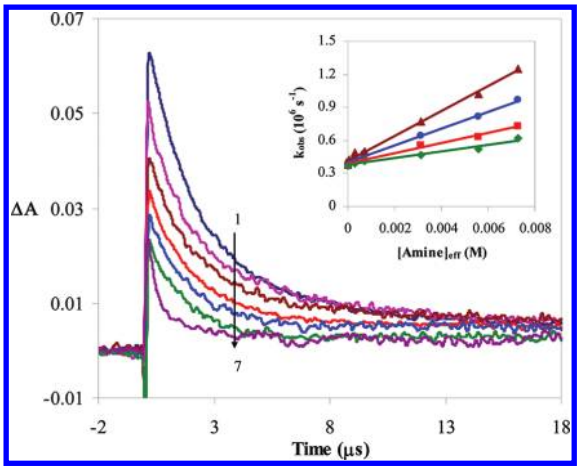

Figure 6. Transient absorption decay of the coumarin radical cation in the presence of different concentrations of EAN in TX-100 micelle monitored at 600 nm. Concentration of EAN: (1) 0, (2) 1.2×10^{-5}, (3) 5.3×10^{-5}, (4) 1.2×10^{-4}, (5) 5.3×10^{-4}, (6) 1.2×10^{-3}, and (7) 5.3×10^{-3} M. The inset shows the plot of observed rate constants (k_{obs}) for the decay of coumarin radical cation versus the concentration of amines in TX-100 micelles: (●) MAN, (■) EAN, (▲) DMAN, and (♦) DEAN.

tration of amines. This indicates that there is a reaction between coumarin radical cation and amines. On the addition of amines, the decay rate constant of hydrated electron does not affected even in the presence of higher concentration of amines (Figure 7). There is no change in the absorbance of the

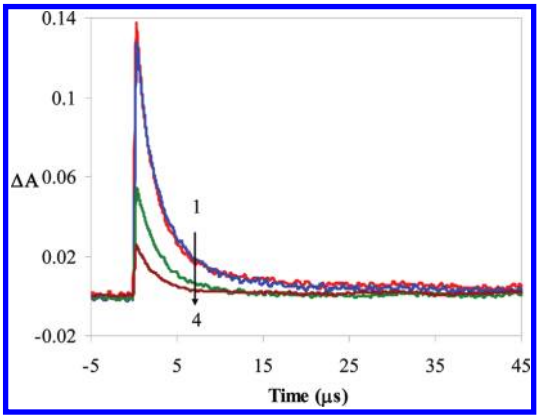

Figure 7. Transient absorption decay of hydrated electron with DMAN in SDS micelles monitored at 710 nm. Concentration of DMAN: (1) 0, (2) 5.3×10^{-3}, (3) 10.2×10^{-3}, and (4) 15.2×10^{-3} M.

hydrated electron on addition of amine up to the concentration of ~5 mM. On further addition of amine, hydrated electron absorbance decreases without change in the decay rate constant. At very high concentration of amine, ultrafast ET is more favorable and competes with the photoionization. Bimolecular quenching rate constants for the reaction of coumarin radical cation with amines were obtained from the slope of the plot of the pseudofirst-order rate constants for decay (k_{obs}) of the appropriate radical cation versus the concentration of amine according to eq 6[44]

$$k_{obs} = k_0 + k_{amine}[\text{amine}] \quad (6)$$

dx.doi.org/10.1021/jp301412c | J. Phys. Chem. B 2012, 116, 4908−4920

where k_0 denote the decay rate of the coumarin radical cation in the absence of amine. The resulting plot shows linear behavior for all C307-amine systems in SDS and TX-100 micelles. The rate constants for the reaction of coumarin radical cation with amines in SDS and TX-100 micelles are listed in Table 7. The

Table 7. Rate Constants for Reaction of the Coumarin Radical Cation with Amines in SDS and TX-100 Micelles, and for Triplet Quenching by Amines in CTAB Micelles

	rate constant for ET between coumarin radical cation and amine (10^6 M^{-1} s^{-1})[a]		rate constant for quenching of coumarin triplet (10^6 M^{-1} s^{-1})[a]
amines	SDS	TX-100	CTAB
MAN	3.95	78.67	6.40
EAN	3.74	47.32	5.54
DMAN	4.06	114.07	8.73
DEAN	3.13	32.77	3.86

[a]Error: ±2%.

bimolecular rate constant for the ET reaction between coumarin radical cation and amine in TX-100 is more than 10 times higher than in SDS micelles. The slow solvent relaxation may facilitate the faster ET reaction in TX-100 micelles. The rate constant for the quenching of coumarin radical cation are in the order of DEAN < EAN < MAN < DMAN.

Transient absorption studies of C307 in the presence of amines in CTAB micelles show different characteristics as compared with other micelles. For all coumarin-amine systems in CTAB micelles, transient spectra exhibit the absorption of amine radical cation (λ_{max} = 450−470 nm) only. The coumarin triplet−triplet absorption (590 and 710 nm) was effectively quenched in the presence of amines, which indicated that the ET takes place to the triplet state. The decay rate constant of coumarin triplet was measured as a function of different concentration of amine in CTAB micelles. Figure 8 shows the transient decay of coumarin triplet monitored at 590 nm with different concentration of DEAN in CTAB micelles. The rate constant for the coumarin triplet decay increases with increase in the concentration of the amine. The bimolecular quenching rate constants for the triplet quenching by amines were obtained from the plot of k_{obs} vs [amine] (inset Figure 8), and tabulated in Table 7. The bimolecular rate constants for triplet quenching in CTAB micelles is increase in the order of DEAN < EAN < MAN < DMAN.

DISCUSSION

The quenching in the S−S fluorescence intensity as well as the decrease in the fluorescence lifetime of C307 on addition of amines can be assigned to the PET from amine to excited C307. It is evident from laser flash photolysis studies, the absorption of amine radical cation confirms that the fluorescence quenching of C307 is attributed to the ET from amine to excited-state of C307 in all micelles. The fluorescence decay of C307 is biexponential in the presence of amine because of the contribution of two kinds of diffusion i.e. (i) diffusion of reactants inside the micelle and (ii) micellar diffusion in the quenching dynamics. The diffusion coefficient of the reactant in the micelles is obtained from fluorescence anisotropy and is found to be in the order of 10^{-9} m^2 s^{-1} whereas the micellar diffusion coefficient obtained from the

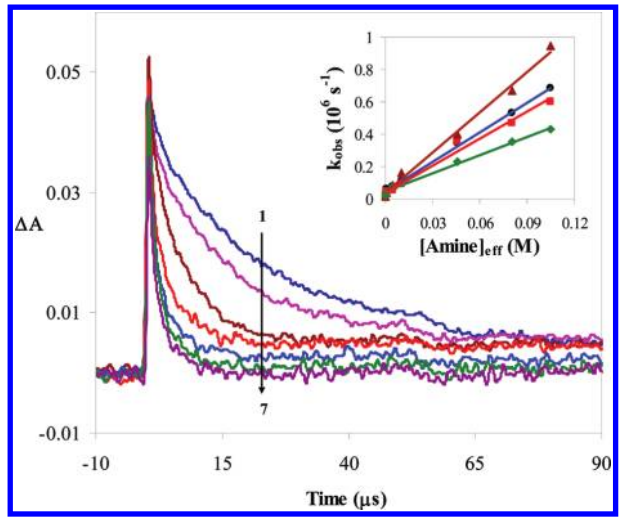

Figure 8. Transient absorption decay of coumarin triplet in the presence of different concentrations of DEAN in CTAB micelle monitored at 590 nm. Concentration of DEAN: (1) 0, (2) 1.2×10^{-5}, (3) 5.3×10^{-5}, (4) 1.2×10^{-4}, (5) 5.3×10^{-4}, (6) 1.2×10^{-3}, and (7) 5.3×10^{-3} M. The inset shows the plot of observed rate constants (k_{obs}) for the decay of coumarin triplet versus the concentration of amines in CTAB micelles: (●) MAN, (■) EAN, (▲) DMAN, and (♦) DEAN.

FCS measurements is found to be in the order of 10^{-10} m^2 s^{-1}.[46] The dynamic quenching ET rate constant is calculated using the average lifetime obtained from the TCSPC measurements. So the dynamic quenching ET rate constants are designated as diffusion averaged dynamic electron transfer [DADET] rate constant and are found to be in the order of 10^9 M^{-1} s^{-1}. The DADET does not affected the solvent relaxation process in SDS and CTAB micelles. This is confirmed by the femtosecond fluorescence decay monitored at the red end of the emission spectrum. The maximum value of the amine concentration used for the DADET was ∼4 mM. Up to this concentration, there is not much change in the rise time observed at 550 nm (and also not much change in the τ_2 time constant monitored at 460 nm). In TX-100 micelle, the rise time observed at 550 nm is almost disappeared at this amine concentration and DADET competes with solvation dynamics. The solvation time of C307 in SDS, CTAB, and TX-100 was reported as 230 ps, 308 ps, and 1.37 ns, respectively.[32] The solvation dynamics is much faster than the DADET in SDS and CTAB micelles whereas DADET is much faster than the solvation dynamics in TX-100 micelles. TX-100 micelles shows higher value of the quenching rate constant (Table 2) and exhibits large difference between the k_q values measured from S-S and T-R fluorescence measurements compared with SDS and CTAB micelles. In all micelles, DADET do not influence the photoionization process which is confirmed by the effect of amine concentration on the hydrated electron absorbance in the concentration range of 0 to 4 mM.

Koch et al.[38] reported that the time dependence of ET rate constant is due to the existence of three different quenching regimes. They are (i) static regime which give intrinsic ET rate constant and is independent of quencher concentration, (ii) nonstationary or transient regime, which depends on the viscosity of the solution, and (iii) stationary regime in which the rate constant is controlled by diffusion of reactant. The static and transient quenching process describes the ultrafast ET is due to the close proximity of C307-amine pairs. There is not

dx.doi.org/10.1021/jp301412c | J. Phys. Chem. B 2012, 116, 4908−4920

much change was observed on the addition of amine in the ultrafast decay time τ_1 monitored at 460 nm, whereas its amplitude increases on the addition of amine. This confirms that the ultrafast decay component (τ_1) is ascribed to the static quenching process and fast decay component (τ_2) is ascribed to the transient quenching process. Ultrafast ET is faster than the solvation, and is calculated from the ultrafast decay component τ_2 monitored at 460 nm. The ultrafast ET rate constants are found to be in the order of 10^{10} s^{-1}. The ultrafast ET was clearly observed in the femtosecond fluorescence decay at higher concentration of amine [5−15 mM]. At higher amine concentration, the number of amine molecules per micelle increases and thereby increases the probability of C307-amine pairs, which are in close proximity. At higher amine concentration, the absence of rise at decay monitored at 550 nm also concludes that the ultrafast quenching process is faster than the solvation.[9] The hydrated electron absorbance decreases with increase in the amine concentration of above 5 mM. This confirms that the ultrafast ET competes with photoionization and decreases the photoionization yield at higher amine concentrations. The ultrafast ET rate constants were found to be ~2×10^{10} s^{-1} irrespective of the nature of the micelles.

The PET reactions between coumarin and aromatic amines have been extensively studied in homogeneous medium.[13,47−50] Satpati et al.[47] studied the ET between C307 and aromatic amines in acetonitrile and reported the k_{et} values in the range of 0.7−1.1 $\times 10^{10}$ M^{-1} s^{-1} for the aromatic amines which used in the present investigation. In micelles, the ET rate constant obtained from S-S and T-R (TCSPC) measurements are 2−4 times lower than the k_{et} values reported in acetonitrile. The diffusive ET is less efficient in micellar medium than the homogeneous medium due to (i) slow diffusion of the donor and acceptor in the micellar phase and (ii) compartmentalization of donor and acceptor. The ultrafast ET rate constants are found to be 2−3 times higher than the rate constant reported in homogeneous solution, and is due to the close proximity of donor and acceptor. The rate constant for DADET is found to depend on the nature of the micelles whereas the ultrafast ET rate constant is similar in all micelles.

Correlation of the ET Rate Constants with the Free Energy Changes. The free energy change (ΔG^0) for the PET reaction between electron donor and electron acceptor is given by the following Rehm−Weller relation[51]

$$\Delta G^0 = E(D/D^+) - E(A/A^-) - E_{00} - \frac{e^2}{\varepsilon_S r_0} \qquad (7)$$

where $E(D/D^+)$ is the oxidation potential of amine, $E(A/A^-)$ is the reduction potential of coumarin, E_{00} is the excitation energy of the coumarin in the S_1 state, e is the electronic charge, ε_S is the dielectric constant of the solvent, and r_0 is the separation between the interacting coumarin and amine molecules. To estimate r_0 values, the individual radii of the donors (r_D) and acceptors (r_A) were estimated using Edward's volume addition method,[52] and r_0 was considered as equal to ($r_D + r_A$). The $E(A/A^-)$, $E(D/D^+)$, and E_{00} values for the present studied are listed in Tables 1 and 8. The dielectric constant of the Stern/palisade layers of the SDS, CTAB, and TX-100 micelles was estimated to be 32, 37.1, and 26, respectively.[35−37]

The estimated ΔG^0 values for coumarin−amine systems in different micelles are also complied in Table 8. The ΔG^0 dependence of ET rate constant of C307 obtained from

Table 8. Reduction Potentials of Amines and ΔG^0 Values for the C307−Amine Systems in Micelles

	$E(D/D^+)$/V (vs SCE)			ΔG^0 (eV)		
amines	SDS	CTAB	TX-100	SDS	CTAB	TX-100
AN	0.77	0.49	0.80	−0.39	−0.94	−0.37
MAN	0.65	0.37	0.68	−0.51	−1.07	−0.49
EAN	0.64	0.36	0.67	−0.52	−1.08	−0.51
DMAN	0.60	0.32	0.63	−0.56	−1.12	−0.55
DEAN	0.56	0.28	0.59	−0.60	−1.16	−0.59

picosecond fluorescence studies (TCSPC) and femtosecond fluorescence studies ($k_{et} = \tau_2^{-1} - \tau_0^{-1}$) in all micelles are shown in Figure 9. An inverse bell-shaped correlation is clearly evident

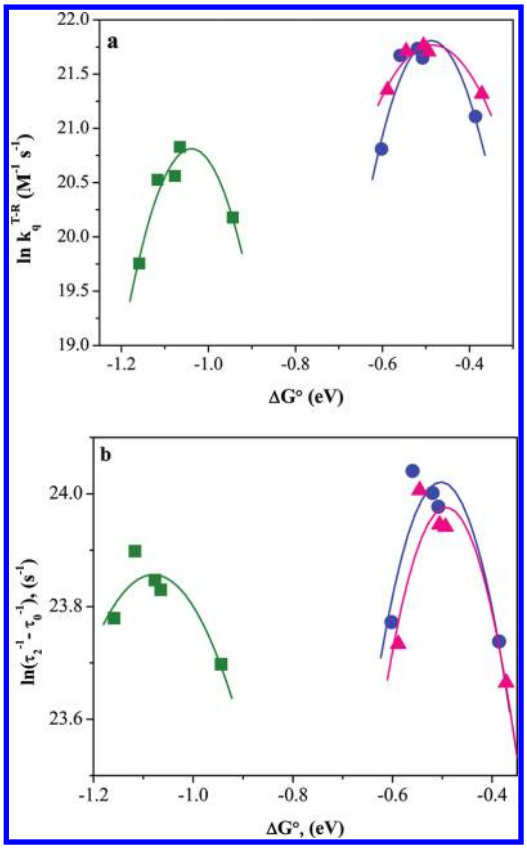

Figure 9. Plot of (a) $\ln(k_q^{T\text{-}R})$ vs ΔG^0, (b) $\ln(\tau_2^{-1} - \tau_0^{-1})$ vs ΔG^0 for C307−amine systems in (●) SDS, (■) CTAB, and (▲) TX-100 micelles. Experimental data are shown by symbols and continuous curves are drawn as the guide to the eyes to represent the trends.

from Figure 9b, and indicates the existence of Marcus inversion in bimolecular ultrafast ET rates in micellar solution. So far, several research groups reported the observation of Marcus inversion for a single electron donor (amine) by varying the electron acceptors (coumarin). To the best of our knowledge, this is the first report on the observation of Marcus inversion for a single electron acceptor (C307) by varying the electron donors (amines). The observed Marcus inversion for the ultrafast ET is identical to that of DADET. As indicated from Figure 9, the inversion in SDS and TX-100 micelles observed at an exergonicity value of ~0.50 eV, and for CTAB micelles an exergonicity value of ~1.05 eV. Substantially higher exergonicity for the Marcus inversion in CTAB micelle was observed as compared with that of SDS and TX-100 micelles. The ET

dx.doi.org/10.1021/jp301412c | J. Phys. Chem. B 2012, 116, 4908−4920

Scheme 2. Excited-State Reactions of C307 in the Presence of Amine in Micelles

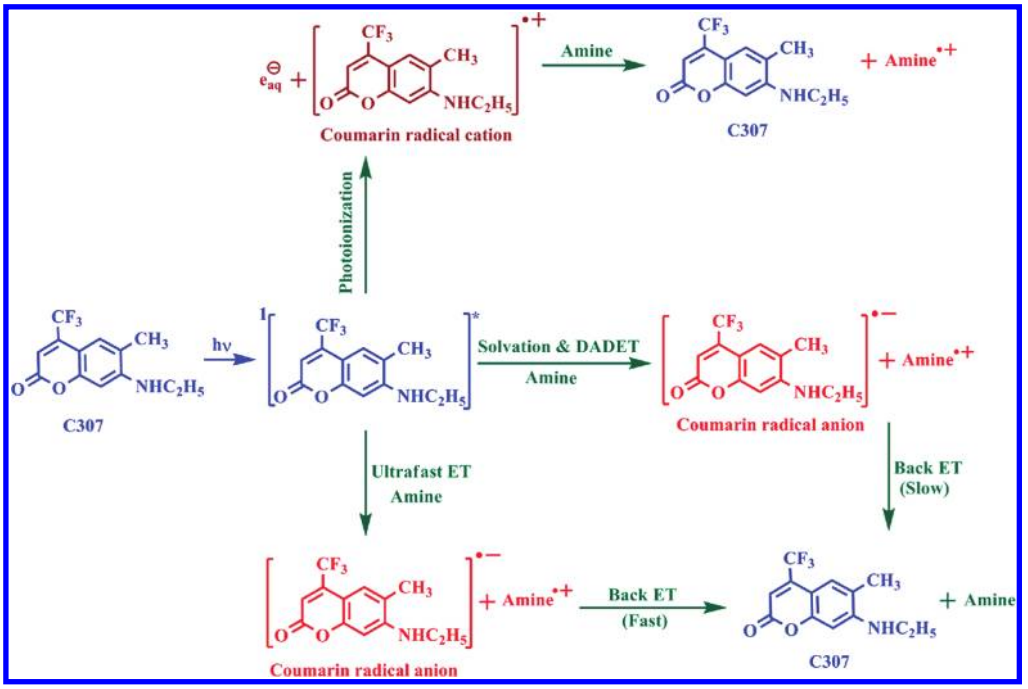

reaction between coumarins and amines under diffusive and nondiffusive conditions was reported by Nad et al.[48] Under diffusive conditions the ET dynamics is governed by solvent reorganization energy, and at higher exergonicity the ET rate constants are leveled off at diffusion controlled rate constant. Under nondiffusive conditions the ET dynamics is controlled by the intramolecular reorganization energy, and inversion in the ET rate constants were observed at higher exergonicity. In the present study, both DADET and ultrafast ET shows Marcus inversion in the ET rate constants at similar exergonicity indicates that the role of diffusion of the reactants inside the micelles and solvent reorganization is negligible toward the activation barrier for the PET in micellar systems used in the present investigation.

The solvent reorganization energy (λ_s) can approximately be estimated using the following expression:[35−37,47,48]

$$\lambda_S = e^2\left\{\frac{1}{2r_D} + \frac{1}{2r_A} - \frac{1}{r}\right\}\left\{\frac{1}{n^2} - \frac{1}{\varepsilon}\right\} \quad (8)$$

where n is the refractive index of micelles (1.33, 1.39, and 1.36 for SDS, CTAB, and TX-100 micelles, respectively),[35−37] ε is the dielectric constant of the solvent, r_D and r_A are the donor and acceptor radius respectively, and r is the separation distance between donor and acceptor. The value of λ_s is estimated to be in the range of ∼1 eV in all micelles. The intramolecular reorganization energy (λ_i) for the coumarin−amine systems is reported to be in the range of about 0.3 eV.[37] Therefore the Marcus inversion in the ET rates in the present systems is expected appear at $-\Delta G^0$ = ∼1.3 eV ($\lambda_s + \lambda_i$ = 1.3 eV). In the present systems Marcus inversion region appears at lower exergonicity in both SDS and TX-100 micelles compared with the calculated ΔG^0 value, whereas in CTAB micelles the observed higher exergonicity is almost similar to that of calculated value. Several groups have reported the similar observation in micelles.[9,43] In micelles, ET occurs under nondiffusive conditions, solvent reorganization energy does not play any significant role on the ET dynamics. This is further supported by the slow solvent reorganization dynamics around the reactants in micelles. The observed solvent relaxation process is slower in TX-100 (∼1.3 ns) compared with that of SDS and CTAB micelles (∼300 ps).[32] The determined ET rate constant in TX-100 micelles is higher than that of SDS and CTAB which indicates that absence of solvent reorganization on the ET dynamics.

Marcus inversion behavior observed in micelles is explained so far based on the distance between donor and acceptor molecules, solvation rates, and intramolecular vibrational motion (2DET) in the micellar medium.[9,35,42] The concentration of C307 (∼10 μM) used in the present study is much lower than the concentration of micelles (∼5 × 10^{-4} M). Hence a single micelle can hold only one or no molecules of C307, whereas single micelles can accommodate more than one amine molecule. On excitation of C307 undergoes both photoionization and ET. In a micelle only one C307 is present, which undergo either photoionization or ET on excitation. DADET may be due to (i) acceptor and donor molecules separated by counterions/alkyl chains in the same micelle (intramicellar quenching) and (ii) donor and acceptor molecules present in two different micelles (intermicellar quenching). The ultrafast ET is due to the intramicellar ET, and the DADET process may be due to the combination of inter- and intramicellar ET. Both ET dynamics is governed by intramolecular reorganization and micellar reorganization energies and not by the solvent reorganization around the reactants in micelles. The observed exergonicity regions are little higher in SDS and TX-100 micelles compared with that of reported intramolecular reorganization energy (0.3 eV). This may be due to the minor role of the micellar reorganization energy on the ET dynamics in SDS and TX-100 micelles. In CTAB micelles, the observed exergonicity region is three times higher than that of reported intramolecular reorganization energy. The observed higher exergonicity may be due to the photoionization and subsequent radical-ion pair recombination. Due to this recombination dynamics the intramolecular

dx.doi.org/10.1021/jp301412c | J. Phys. Chem. B 2012, 116, 4908−4920

reorganization energy may be higher than the reported value in CTAB micelles.

In order to understand the role of diffusion on ET, the diffusion distance ($(2D_t\tau)^{1/2}$) of coumarin dye along the micellar surface is calculated by using diffusion coefficient of C307 in micelles.[9,53] The diffusion coefficient of C307 in micelles is obtained by T-R fluorescence anisotropy decay.[32] The values of the translational diffusion coefficient of C307 in SDS, CTAB, and TX-100 micelles are found to be 2.35×10^{-9}, 0.81×10^{-9}, and 4.03×10^{-9} m^2 s^{-1}, respectively, by using wobbling-in-cone model. The average decay time of C307 (ultrafast ET) in the presence of highest concentration of amines (~15 mM) is used as τ (Supporting Information, Table S1). The estimated diffusion distances in all micelles are found to be ~3 Å, which is less than the sum of the radius of the electron donor and acceptor used in the present investigation. This confirms the donor and acceptor are in close contact in the case of ultrafast ET. The diffusion distance for DADET process in all micelles is determined using picosecond fluorescence quenching data, and the average lifetime in the presence of 4 mM concentration of amines is used as τ. The diffusion distances are estimated in the range of ~30, 20, and 50 Å for SDS, CTAB, and TX-100 micelles, respectively (Supporting Information, Table S1). These diffusion distances are very similar to the radius of the respective micelles. This indicates that the DADET may also be due to intermicellar ET process where the donor molecule located at the peripheral of a micelle and acceptor molecule located at the peripheral of another micelle.

To the best of our knowledge, this is the first report that correlates S-S, T-R fluorescence, and the transient absorption studies to the ET reaction for the coumarin probe in micellar media. The mechanism of the excited-state reactions of C307 in the presence of an electron donors is depicted in Scheme 2. The photoionization of C307 leads to the formation of coumarin radical cation and hydrated electron. The coumarin radical cation reacts with amine molecules results in the formation of ground-state coumarin and amine radical cation. The reaction of amine with the coumarin radical cation is confirmed by the effect of amine concentration on the decay of the coumarin radical cation at 610 nm. The regeneration of ground-state coumarin by the above reaction is confirmed by the bleach recovery monitored at 410 nm in the presence of amine. The bleach recovery of C307 in CTAB monitored at 410 nm in the absence and presence of different concentration of DMAN is shown in Figure 10.

The bleach at 410 nm is due to the depletion of ground-state C307 by the laser pulse. In the absence of amine, the strong ground-state bleach is due to the photoionization of C307 by the laser pulse and the bleach recovery is due to regeneration of ground-state C307 by the recombination of radical cation and hydrated electron and transfer of population from triplet state to ground-state. In the presence of amines, decrease in the bleach is due to ultrafast recovery of ground-state C307 by ultrafast back electron transfer. The ultrafast ET takes place in less than 75 ps in all of the micelles, which is an intramicellar process, so the back ET is more favorable. The back ET may take place in less than 200 ps in all of the micelles. McArthur et al. have reported 163 ps for the back ET between coumarin 314 and DMAN at an organic liquid and aqueous interface.[54] The probability of ultrafast forward and back ET increases with increasing concentration of amine which results in the ultrafast recovery of ground-state C307. This ultrafast recovery is not

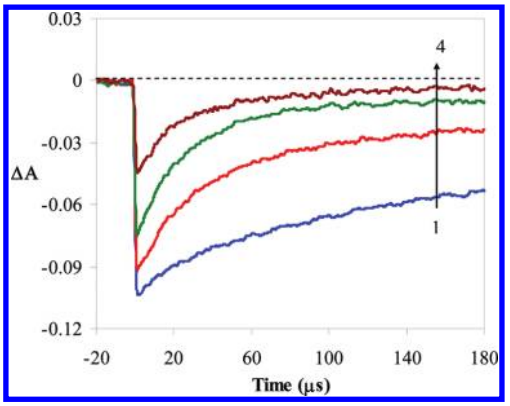

Figure 10. Ground-state bleach recovery of C307 in the absence and presence of DMAN in CTAB micelle monitored at 410 nm. Concentration of DMAN: (1) 0, (2) 1.2×10^{-5}, (3) 5.3×10^{-5}, and (4) 5.3×10^{-4} M.

observed due to the finite time resolution (8 ns) of the nanosecond transient absorption setup. The observed slow ground-state recovery of C307 (in microsecond time scale) is due to (1) ET reaction between amine and coumarin radical cation and (2) back electron transfer. The multiexponential recovery of ground-state C307 in the presence of amine indicates more than one mechanism operating for the recovery of ground-state. The rate constant for the reaction of amine with coumarin radical cation is found to be in the order of 10^7 M^{-1} s^{-1}, this is responsible for the recovery of ground-state C307 in the microsecond time scale. The back electron transfer is very slow due to the intermicellar DADET processes, which leads to the efficient separation of coumarin radical anion and amine radical cation. The residual bleach observed after 150 μs may be due to the slow back ET, which may be completed in milliseconds time scale.

On the basis of the above discussion, we proposed the entirely new fact for the explanation of the upward curvature observed in the steady-state S−V plot. So far, all the reports consider only the static and transient quenching process for the upward curvature of the S−V plot at higher concentration of amine.[30,35,38] At low concentration of amine, coumarin radical cation scavenges the amines effectively thereby reducing the effective quencher concentration in micelles. The quenching efficiency increases nonlinearly with increasing amine concentrations. In addition to static and transient quenching, the reaction between the coumarin radical cation and amine may also be one of the reasons for the upward curvature in the S−V plot.

The ultrafast ET reactions between excited coumarin and amine lead to the formation of the coumarin radical anion and amine radical cation. Ultrafast ET results by the close contact of donor and acceptor pairs, so the back ET is efficient which results back in the ground-state C307 and amine. DADET reaction also results in the formation of coumarin radical anion and amine radical cation. DADET process occurs between donor and acceptor molecules where these molecules are located in the same single micelle which is separate by micellar headgroups and counterions (intramicelle), and also both are located in different micelles separately (intermicelle). For the intramicellar case, the back ET of coumarin radical anion and amine radical cation is occurring fast, whereas the slow back ET process takes place for the intermicellar case. This is confirmed by the transient decay of amine radical cation which was

dx.doi.org/10.1021/jp301412c | J. Phys. Chem. B 2012, 116, 4908−4920

monitored at respective wavelength (~460 nm) in the presence of different amine concentrations (Supporting Information, Figure S2). The transient decays of the amine radical cation have short-lived and long-lived components for all coumarin−amine systems in all micelles. This short-lived component is due to the intramicellar recombination of radical-ion pair and long-lived component is due to the intermicellar recombination of radical-ion pair. Nad et al. reported that the transient absorption of coumarin radical anion is observed at 720 nm in acetonitrile using pulse radiolysis.[55] In the present systems, the coumarin radical anion could not be observed clearly due to overlap of hydrated electron absorption in the same region and recombination of the coumarin radical anion and the amine radical cation. The present investigation confirms the following three different PET processes for C307−amine systems in all micelles. They are (1) ET to the excited Franck−Condon state of C307, (2) ET to the relaxed excited-state of C307, and (3) ET to the coumarin radical cation generated by photoionization. Out of the above three ET processes, the ET to the relaxed excited-state of C307 may be important for practical application such as solar energy conversion and storage due to the long-lived charge separated radical ions.

CONCLUSION

The PET reactions between the excited C307 and amines in micelles have been investigated using S-S and T-R absorption and fluorescence measurements. Based on the fluorescence quenching time scale, PET in micelles is grouped into two types, (i) ultrafast ET due to the close contact of the donor and acceptor in micelles and (ii) DADET, which is controlled by the diffusion of reactant in micellar Stern layer and diffusion of the micelles. The ultrafast ET is faster than the solvation and competes with photoionization in the Franck−Condon state. In all micelles, the rate constant for the DADET is 10 times smaller than those reported in homogeneous solution. DADET is slower than the solvent relaxation in SDS and CTAB micelles and is faster than solvent relaxation in TX-100 micelle. DADET do not influence the photoionization of C307 in all micelles. Both ultrafast and DADET quenching rate constants in all micellar media show the Marcus inversion behavior on plotting the ET rate constants against ΔG^0. Both ET processes exhibit inversion in the ET rate at the exergonicity of ~0.5, 1.05, and 0.5 eV in SDS, CTAB, and TX-100 micelles, respectively. This concludes that the role of diffusion of reactants and solvent reorganization energies toward the activation barrier for ET reactions in micelles is negligible. The ultrafast and DADET dynamics is governed by intramolecular and micellar reorganization energies in all micelles. The observed higher exergonicity in CTAB micelles can be due to the photoionization and subsequent radical-ion pair recombination results in the triplet state, which need high intramolecular reorganization energy.

PET from amine to the excited-state C307 is confirmed by the observation of amine radical cation absorption in the laser flash photolysis. The ET reaction between the coumarin radical cation generated by the photoionization and amine is demonstrated first time in the coumarin-amine system. The decrease in the ground-state bleach and faster recovery of the ground-state absorption of C307 at 410 nm in the presence of amines confirms the regeneration of ground-state coumarin through the fast back electron transfer and reaction of amine with coumarin radical cation. Mechanism for the PET reaction between C307−amine systems is proposed for the first time in micelles including photoionization, ultrafast and dynamic ET, and solvation dynamics.

ASSOCIATED CONTENT

Supporting Information

Femtosecond fluorescence transient decay of C307 with different concentrations of DMAN in micelles monitored at red edge (550 nm); the table consists of the estimated diffusion distances and average lifetimes for C307−amine systems in micelles; transient absorption decay of amine radical cation in the presence of different concentrations of DMAN in SDS micelle. This material is available free of charge via the Internet at http://pubs.acs.org.

AUTHOR INFORMATION

Corresponding Author

*E-mail: selvaraj24@hotmail.com.

Notes

The authors declare no competing financial interest.

ACKNOWLEDGMENTS

We thank Prof. P. Ramamurthy for many informative discussions during the course of this work. This work was supported by University Grants Commission, Government of India by Grant No. 31-138/2005(SR) to C.S.

REFERENCES

(1) Hamley, I. W. *Introduction to Soft Matter: Synthetic and Biological Self-Assembling Materials*; John Wiley & Sons, Ltd.: London, England, 2007.
(2) Piazza, R. *Soft Matter: The Stuff That Dreams Are Made Of*; Springer-Verlag: Italia, 2010.
(3) Pelizetti, M.; Schiavello, M. *Photochemical Conversion and Storage of Solar Energy*; Kluwer: Dordrecht, Germany, 1997.
(4) O'Regan, B.; Gratzel, M. *Nature* **1991**, *353*, 737−740.
(5) Graztal, M. *Heterogeneous photochemical Electron Transfer*; CRC Press: Boca Raton, FL, 1989.
(6) Pal, S. K.; Mandal, D.; Sukul, D.; Bhattacharyya, K. *Chem. Phys.* **1999**, *249*, 63−71.
(7) Nanda, J.; Behera, P. K.; Tavernier, H. L.; Fayer, M. D. *J. Lumin.* **2005**, *115*, 138−146.
(8) Kumbhakar, M.; Singh, P. K.; Satpati, A. K.; Nath, S.; Pal, H. *J. Phys. Chem. B* **2010**, *114*, 10057−10065.
(9) Ghosh, S.; Mondal, S. K.; Sahu, K.; Bhattacharyya, K. *J. Chem. Phys.* **2007**, *126*, 204708−1−11.
(10) Yoshihara, K. *Adv. Chem. Phys.* **1999**, *107*, 371−402.
(11) Kobayashi, T.; Takagi, Y.; Kandori, H.; Kemnitz, K.; Yoshihara, K. *Chem. Phys. Lett.* **1991**, *180*, 416−422.
(12) Pal, H.; Nagasawa, Y.; Tominaga, K.; Yoshihara, K. *J. Phys. Chem.* **1996**, *100*, 11964−11974.
(13) Shirota, H.; Pal, H.; Tominaga, K.; Yoshihara, K. *J. Phys. Chem. A* **1998**, *102*, 3089−3102.
(14) Akesson, E.; Johnson, A. E.; Levinger, N. E.; Walker, G. C.; DuBruil, T. P.; Barbara, P. F. *J. Chem. Phys.* **1992**, *96*, 7859−7862.
(15) Bagchi, B.; Gayathri, N. *Adv. Chem. Phys.* **1999**, *107*, 1−80.
(16) Roy, S.; Bagchi, B. *J. Phys. Chem.* **1994**, *98*, 9207−9215.
(17) Ghosh, S.; Sahu, K.; Mondal, S. K.; Sen, P.; Bhattacharyya, K. *J. Chem. Phys.* **2006**, *125*, 054509−1−7.
(18) Marcus, R. A. *J. Chem. Phys.* **1956**, *24*, 966−978.
(19) Newton, M. D.; Sutin, N. *Annu. Rev. Phys. Chem.* **1984**, *35*, 437−480.
(20) Marcus, R. A. *Angew. Chem., Int. Ed. Engl.* **1993**, *32*, 1111−1121.
(21) Sumi, H.; Marcus, R. A. *J. Chem. Phys.* **1986**, *84*, 4894−4914.
(22) Yoshihara, K.; Tominaga, K.; Nagasawa, Y. *Bull. Chem. Soc. Jpn.* **1995**, *68*, 696−712.

(23) Chakraborty, A.; Seth, D.; Setua, P.; Sarkar, N. *J. Chem. Phys.* **2008**, *128*, 204510−1−9.
(24) Kumbhakar, M.; Mukherjee, T.; Pal, H. *Chem. Phys. Lett.* **2005**, *410*, 94−98.
(25) Kumbhakar, M.; Nath, S.; Mukherjee, T.; Pal, H. *J. Photchem. Photobiol., A* **2006**, *182*, 7−16.
(26) Chakraborty, A.; Chakrabarty, D.; Hazra, P.; Seth, D.; Sarkar, N. *Chem. Phys. Lett.* **2003**, *382*, 508−517.
(27) Chakraborty, A.; Seth, D.; Seth, P.; Sarkar, N. *J. Phys. Chem. B* **2006**, *110*, 16607−16617.
(28) Tablet, C.; Matei, I.; Hillebrand, M. *J. Mol. Liq.* **2011**, *160*, 57−62.
(29) Das, A. K.; Mondal, T.; Mojumdar, S. S.; Bhattacharyya, K. *J. Phys. Chem. B* **2011**, *115*, 4680−4688.
(30) Sarkar, S.; Mandal, S.; Pramanik, R.; Ghatak, C.; Rao, V. G.; Sarkar, N. *J. Phys. Chem. B* **2011**, *115*, 6100−6110.
(31) Sarkar, S.; Pramanik, R.; Ghatak, C.; Rao, V. G.; Sarkar, N. *Chem. Phys. Lett.* **2011**, *506*, 211−216.
(32) Dhenadhayalan, N.; Selvaraju, C.; Ramamurthy, P. *J. Phys. Chem. B* **2011**, *115*, 10892−10902.
(33) Kalyanasundaram, K. *Photochemistry in Microheterogeneous System*; Academic Press: Orlando, FL, 1987.
(34) Tavernier, H. L.; Laine, F.; Fayer, M. D. *J. Phys. Chem. A* **2001**, *105*, 8944−8957.
(35) Kumbhakar, M.; Nath, S.; Mukherjee, T.; Pal, H. *J. Chem. Phys.* **2004**, *120*, 2824−2834.
(36) Kumbhakar, M.; Nath, S.; Pal, H.; Sapre, A. V.; Mukherjee, T. *J. Chem. Phys.* **2003**, *119*, 388−399.
(37) Kumbhakar, M.; Nath, S.; Mukherjee, T.; Pal, H. *J. Chem. Phys.* **2005**, *123*, 034705−1−11.
(38) Koch, M.; Rosspeintner, A.; Angulo, G.; Vauthey, E. *J. Am. Chem. Soc.* **2012**, *134*, 3729−3736.
(39) Lakowicz, J. R. *Principles of Fluorescence Spectroscopy*, 3rd ed.; Springer: New York, 2006.
(40) Infelta, P. P.; Gratzel, M.; Thomas, J. K. *J. Phys. Chem.* **1974**, *78*, 190−195.
(41) Tachiya, M. *Can. J. Phys.* **1990**, *68*, 979−991.
(42) Satpati, A. K.; Kumbhakar, M.; Nath, S.; Pal, H. *J. Photochem. Photobiol., A* **2008**, *200*, 270−276.
(43) Kumbhakar, M.; Singh, P. K.; Nath, S.; Bhasikuttan, A. C.; Pal, H. *J. Phys. Chem. B* **2008**, *112*, 6646−6652.
(44) Workentin, M. S.; Johnston, L. J.; Wayner, D. D. M.; Parker, V. D. *J. Am. Chem. Soc.* **1994**, *116*, 8279−8287.
(45) Chowdhury, A.; Basu, S. *J. Lumin.* **2006**, *121*, 113−122.
(46) Dey, S.; Mandal, U.; Mojumdar, S. S.; Mandal, A. K.; Bhattacharyya, K. *J. Phys. Chem. B* **2010**, *114*, 15506−15511.
(47) Satpati, A. K.; Nath, S.; Kumbhakar, M.; Maity, D. K.; Senthilkumar, S.; Pal, H. *J. Mol. Struct.* **2008**, *878*, 84−94.
(48) Nad, S.; Pal, H. *J. Phys. Chem. A* **2000**, *104*, 673−680.
(49) Tablet, C.; Hillebrand, M. *J. Photochem. Photobiol., A* **2007**, *189*, 73−79.
(50) Castner, E. W., Jr.; Kennedy, D.; Cave, R. J. *J. Phys. Chem. A* **2000**, *104*, 2869−2885.
(51) Rehm, D.; Weller, A. *Isr. J. Chem.* **1970**, *8*, 259−271.
(52) Edwards, J. T. *J. Chem. Educ.* **1970**, *47*, 261−270.
(53) Mondal, S. K.; Ghosh, S.; Sahu, K.; Mandal, U.; Bhattacharyya, K. *J. Chem. Phys.* **2006**, *125*, 224710−1−9.
(54) McArthur, E. A.; Eisenthal, K. B. *J. Am. Chem. Soc.* **2006**, *128*, 1068−1069.
(55) Nad, S.; Pal, H. *J. Photochem. Photobiol., A* **2000**, *134*, 9−15.